Variational Continual Learning

Cuong V. Nguyen Yingzhen Li Thang D. Bui Richard E. Turner

Department of Engineering, University of Cambridge
{vcn22,yl494,tdb40,ret26}@cam.ac.uk

Abstract

This paper develops variational continual learning (VCL), a simple but general framework for continual learning that fuses online variational inference (VI) and recent advances in Monte Carlo VI for neural networks. The framework can successfully train both deep discriminative models and deep generative models in complex continual learning settings where existing tasks evolve over time and entirely new tasks emerge. Experimental results show that variational continual learning outperforms state-of-the-art continual learning methods on a variety of tasks, avoiding catastrophic forgetting in a fully automatic way.

1 Introduction

Continual learning (also called life-long learning and incremental learning) is a very general form of online learning in which data continuously arrive in a possibly non i.i.d. way, tasks may change over time (e.g. new classes may be discovered), and entirely new tasks can emerge (Schlimmer and Fisher, 1986; Sutton and Whitehead, 1993; Ring, 1997). What is more, continual learning systems must adapt to perform well on the entire set of tasks in an online way that avoids revisiting all previous data at each stage. This is a key problem in machine learning since real world tasks continually evolve over time (e.g. they suffer from covariate and dataset shift) and the size of datasets often prohibits frequent batch updating. Moreover, practitioners are often interested in solving a set of related tasks that benefit from being handled jointly in order to leverage multi-task transfer. Continual learning is also of interest to cognitive science, being an intrinsic human ability.

The ubiquity of deep learning means that it is important to develop deep continual learning methods. However, it is challenging to strike a balance between adapting to recent data and retaining knowledge from old data. Too much plasticity leads to the infamous catastrophic forgetting problem (McCloskey and Cohen, 1989; Ratcliff, 1990; Goodfellow et al., 2014a) and too much stability leads to an inability to adapt. Recently there has been a resurgence of interest in this area. One approach trains individual models on each task and then carries out a second stage of training to combine them (Lee et al., 2017). A more elegant and more flexible approach maintains a single model and uses a single type of regularized training that prevents drastic changes in the parameters which have a large influence on prediction, but allows other parameters to change more freely (Li and Hoiem, 2016; Kirkpatrick et al., 2017; Zenke et al., 2017). The approach developed here follows this venerable work, but is arguably more principled, extensible and automatic.

This paper is built on the observation that there already exists an extremely general framework for continual learning: Bayesian inference. Critically, Bayesian inference retains a distribution over model parameters that indicates the plausibility of any setting given the observed data. When new data arrive, we combine what previous data have told us about the model parameters (the previous posterior) with what the current data are telling us (the likelihood). Multiplying and renormalizing yields the new posterior, from which point we can recurse. Critically, the previous posterior constrains parameters that strongly influence prediction, preventing them from changing drastically, but it allows other parameters to change. The wrinkle is that exact Bayesian inference is typically intractable and so approximations are required. Fortunately, there is an extensive literature on approximate inference for neural networks. We merge online variational inference (VI) (Ghahramani and Attias, 2000; Sato, 2001; Broderick et al., 2013) with Monte Carlo VI for neural networks (Blundell et al., 2015) to yield *variational continual learning* (VCL). In addition, we extend

VCL to include a small episodic memory by combining VI with the coreset data summarization method (Bachem et al., 2015; Huggins et al., 2016). We demonstrate that the framework is general, applicable to both deep discriminative models and deep generative models, and that it yields excellent performance.

2 Continual Learning by Approximate Bayesian Inference

Consider a discriminative model that returns a probability distribution over an output y given an input $\boldsymbol{x}$ and parameters $\boldsymbol{\theta}$, that is $p(y|\boldsymbol{\theta}, \boldsymbol{x})$. Below we consider the specific case of a softmax distribution returned by a neural network with weight and bias parameters, but we keep the development general for now. In the continual learning setting, the goal is to learn the parameters of the model from a set of sequentially arriving datasets $\{\boldsymbol{x}_t^{(n)}, y_t^{(n)}\}_{n=1}^{N_t}$ where, in principle, each might contain a single datum, $N_t = 1$. Following a Bayesian approach, a prior distribution $p(\boldsymbol{\theta})$ is placed over $\boldsymbol{\theta}$. The posterior distribution after seeing T datasets is recovered by applying Bayes' rule:

$$p(\boldsymbol{\theta}|\mathcal{D}_{1:T}) \propto p(\boldsymbol{\theta}) \prod_{t=1}^{T} \prod_{n_t=1}^{N_t} p(y_t^{(n_t)}|\boldsymbol{\theta}, \boldsymbol{x}_t^{(n_t)}) = p(\boldsymbol{\theta}) \prod_{t=1}^{T} p(\mathcal{D}_t|\boldsymbol{\theta}) \propto p(\boldsymbol{\theta}|\mathcal{D}_{1:T-1}) p(\mathcal{D}_t|\boldsymbol{\theta}).$$

Here the input dependence has been suppressed on the right hand side to lighten notation. We have used the shorthand $\mathcal{D}_t = \{y_t^{(n)}\}_{n=1}^{N_t}$. Importantly, a recursion has been identified whereby the posterior after seeing the T-th dataset is produced by taking the posterior after seeing the $(T-1)$-th dataset, multiplying by the likelihood and renormalizing. In other words, online updating emerges naturally from Bayes' rule.

In most cases the posterior distribution is intractable and approximation is required, even when forming the first posterior $p(\boldsymbol{\theta}|\mathcal{D}_1) \approx q_1(\boldsymbol{\theta}) = \text{proj}(p(\boldsymbol{\theta})p(\mathcal{D}_1|\boldsymbol{\theta}))$. Here $q(\boldsymbol{\theta}) = \text{proj}(p^*(\boldsymbol{\theta}))$ denotes a projection operation that takes the intractable un-normalized distribution $p^*(\boldsymbol{\theta})$ and returns a tractable normalized approximation $q(\boldsymbol{\theta})$. The field of approximate inference provides several choices for the projection operation including i) Laplace approximation, ii) variational KL minimization, iii) moment matching, and iv) importance sampling. Having approximated the first posterior distribution, subsequent approximations can be produced recursively by combining the approximate posterior distribution with the likelihood and projecting, that is $p(\boldsymbol{\theta}|\mathcal{D}_{1:T}) \approx q_T(\boldsymbol{\theta}) = \text{proj}(q_{T-1}(\boldsymbol{\theta})p(\mathcal{D}_T|\boldsymbol{\theta}))$. In this way online updating is supported. This general approach leads, for the four projection operators previously identified, to i) Laplace propagation (Smola et al., 2004), ii) online VI (Ghahramani and Attias, 2000; Sato, 2001) also known as streaming VB (Broderick et al., 2013), iii) assumed density filtering (Maybeck, 1982) and iv) sequential Monte Carlo (Liu and Chen, 1998). In this paper the online VI approach is used as it typically outperforms the other methods for complex models in the static setting (Bui et al., 2016) and yet it has not been applied to continual learning of neural networks.

2.1 Variational Continual Learning (VCL) and Episodic Memory Enhancement

Variational continual learning employs a projection operator defined through a KL divergence minimization over the set of allowed approximate posteriors $\mathcal{Q}$,

$$q_t(\boldsymbol{\theta}) = \arg\min_{q \in \mathcal{Q}} \text{KL}\Big(q(\boldsymbol{\theta}) \parallel \frac{1}{Z_t} q_{t-1}(\boldsymbol{\theta})\ p(\mathcal{D}_t|\boldsymbol{\theta})\Big), \text{ for } t = 1, 2, \ldots, T. \tag{1}$$

The zeroth approximate distribution is defined to be the prior, $q_0(\boldsymbol{\theta}) = p(\boldsymbol{\theta})$. Z_t is the intractable normalizing constant of $p^*(\boldsymbol{\theta}) = q_{t-1}(\boldsymbol{\theta})\ p(\mathcal{D}_t|\boldsymbol{\theta})$ and is not required to compute the optimum.

VCL will perform exact Bayesian inference if the true posterior is a member of the approximating family, $p(\boldsymbol{\theta}|\mathcal{D}_1, \mathcal{D}_2, \ldots, \mathcal{D}_t) \in \mathcal{Q}$ at every step t. Typically this will not be the case and we might worry that performing repeated approximations may accumulate errors causing the algorithm to forget old tasks. Furthermore, the minimization at each step is also approximate (e.g. due to employing an additional Monte Carlo approximation) and so additional information may be lost. In order to mitigate this potential problem, we extend VCL to include a small representative set of data from previously observed tasks that we call the coreset. The coreset is analogous to an episodic memory that retains key information (in our case, important training data points) from previous tasks which the algorithm can revisit in order to refresh its memory of

Algorithm 1 Coreset VCL

Input: Prior $p(\boldsymbol{\theta})$, coreset size K from each task.
Output: Variational and predictive distributions at each step $\{q_t(\boldsymbol{\theta}), p(y^*|\boldsymbol{x}^*, \mathcal{D}_{1:t})\}_{t=1}^T$.

Initialize the coreset and variational approximation: $C_0 \leftarrow \emptyset$, $q_0 \leftarrow p_0$.
for $t = 1 \dots T$ **do**
  Observe the next dataset $\mathcal{D}_t$.
  $C_t \leftarrow$ update the coreset using C_{t-1} and $\mathcal{D}_t$.
  Update the variational distribution for non-coreset data points:

$$\tilde{q}_t(\boldsymbol{\theta}) \leftarrow \arg\min_{q \in \mathcal{Q}} \mathrm{KL}\big(q(\boldsymbol{\theta}) \parallel \tfrac{1}{Z}\tilde{q}_{t-1}(\boldsymbol{\theta})\, p(\mathcal{D}_t \cup C_{t-1} \setminus C_t|\boldsymbol{\theta})\big). \tag{2}$$

  Compute the final variational distribution (only used for prediction, and not propagation):

$$q_t(\boldsymbol{\theta}) \leftarrow \arg\min_{q \in \mathcal{Q}} \mathrm{KL}\big(q(\boldsymbol{\theta}) \parallel \tfrac{1}{Z}\tilde{q}_t(\boldsymbol{\theta}) p(C_t|\boldsymbol{\theta})\big). \tag{3}$$

  Perform prediction at test input $\boldsymbol{x}^*$: $p(y^*|\boldsymbol{x}^*, \mathcal{D}_{1:t}) = \int q_t(\boldsymbol{\theta}) p(y^*|\boldsymbol{\theta}, \boldsymbol{x}^*) \mathrm{d}\boldsymbol{\theta}$.
end for

them. This idea of using an episodic memory has been explored for continual learning by Lopez-Paz and Ranzato (2017).

Algorithm 1 describes coreset VCL. The algorithm maintains a pair $(C_t, \tilde{q}_t)$ comprising the coreset and the variational distribution for non-coreset data at each time step t. The distribution $\tilde{q}_t$ is continuously updated using eq. (2). When performing prediction, $\tilde{q}_t$ and C_t are combined to form the final variational distribution q_t using eq. (3). This step ensures recent exposure to data from each task and helps mitigate any residual forgetting. The coreset VCL algorithm adds new data points to the coreset after observing each new dataset $\mathcal{D}_t$ (it is simple to remove them too if T is large). Any method can be used to update the coreset. For example, K data points can be selected at random from $\mathcal{D}_t$ and added to C_{t-1} to form an unbiased new coreset C_t. Alternatively, the greedy K-center algorithm (Gonzalez, 1985) can be used to return K data points that are guaranteed to be spread throughout the input space.

3 Variational Continual Learning in Deep Discriminative Models

The VCL framework is general and can be applied to many discriminative probabilistic models. Here we apply it to continual learning of deep fully-connected neural network classifiers. Before turning to the application of VCL, we first consider the architecture of neural networks suitable for performing continual learning. In simple instances of discriminative continual learning, where data are arriving in an i.i.d. way or where only the input distribution $p(\boldsymbol{x}_{1:T})$ changes over time, a standard *single-head* discriminative neural network suffices. In many cases, the tasks, although related, might involve different output variables. Standard practice in multi-task learning (Bakker and Heskes, 2003) uses networks that share parameters close to the inputs but with separate heads for each output, hence *multi-head* networks. Graphical models depicting the network architecture for deep discriminative and deep generative models are shown in fig. 1. A general solution to continual learning would perform automatic model building that adds new structure to the existing model as new tasks are encountered (Rusu et al., 2016). Although this is an interesting research direction, here we make the simplifying assumption that the model structure is known *a priori*.

VCL requires specification of $q(\boldsymbol{\theta})$ where $\boldsymbol{\theta}$ in the current case is a D dimensional vector formed by stacking the network's biases and weights. For simplicity we use a Gaussian mean-field approximate posterior $q_t(\boldsymbol{\theta}) = \prod_{d=1}^D \mathcal{N}(\theta_{t,d}; \mu_{t,d}, \sigma_{t,d}^2)$. Taking the most general case of a multi-head network, before task k is encountered the posterior distribution over the associated head parameters will remain at the prior and so $q(\boldsymbol{\theta}_k^H) = p(\boldsymbol{\theta}_k^H)$. This is convenient as it means the variational approximation can be grown incrementally, starting from the prior, as each task emerges. Moreover, only tasks present in the current dataset $\mathcal{D}_t$ need to have their posterior distributions over head parameters updated. The shared parameters, on the other hand, will be constantly updated. Training the network using the VFE approach in eq. (1) is equivalent to maximizing the negative online variational free energy or the variational lower bound to the online marginal

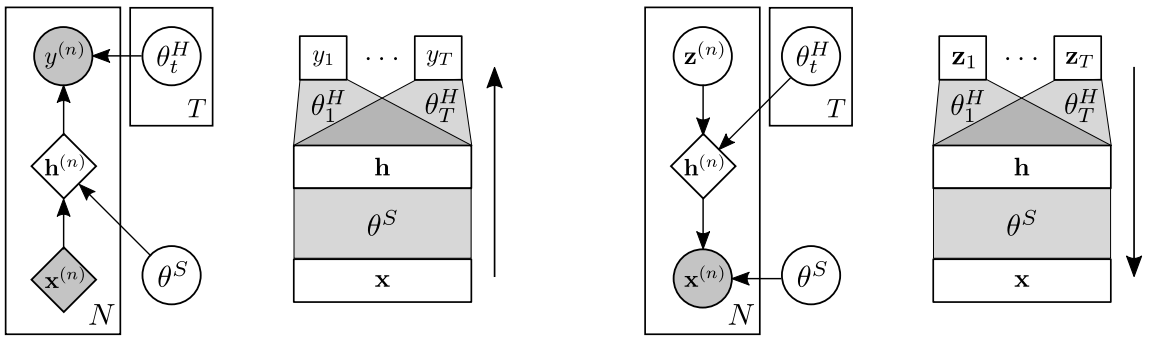

(a) multi-head discriminative network

(b) multi-head generative network

Figure 1: Visualizations of the multi-head networks tested in the paper, including both graphical model (left) and network architecture (right) illustrations. (a) A multi-head discriminative model showing how network parameters might be shared during training. The lower-level network is parameterized by the variables $\boldsymbol{\theta}^S$ and is shared across multiple tasks. Each task t has its own "head network" $\boldsymbol{\theta}_t^H$ mapping to the outputs from a common hidden layer. The full set of parameters is therefore $\boldsymbol{\theta} = \{\boldsymbol{\theta}_{1:T}^H, \boldsymbol{\theta}^S\}$. (b) A multi-head generative model with shared network parameters. The head networks generate the intermediate level representations from the latent variables $\mathbf{z}$.

likelihood:

$$\mathcal{L}_{\text{VCL}}^t(q_t(\boldsymbol{\theta})) = \sum_{n=1}^{N_t} \mathbb{E}_{\boldsymbol{\theta}\sim q_t(\boldsymbol{\theta})}\left[\log p(y_t^{(n)}|\boldsymbol{\theta}, \mathbf{x}_t^{(n)})\right] - \text{KL}(q_t(\boldsymbol{\theta})||q_{t-1}(\boldsymbol{\theta})) \tag{4}$$

with respect to the variational parameters $\{\mu_{t,d}, \sigma_{t,d}\}_{d=1}^D$. Whilst the KL-divergence $\text{KL}(q_t(\boldsymbol{\theta})||q_{t-1}(\boldsymbol{\theta}))$ can be computed in closed-form, the expected log-likelihood requires further approximation. Here we take the usual approach of employing simple Monte Carlo and use the *reparameterization* trick to compute the gradients (Salimans and Knowles, 2013; Kingma and Welling, 2014). At the first time step, the prior distribution, and therefore $q_0(\boldsymbol{\theta})$ is chosen to be a multivariate Gaussian distribution (see e.g. Graves, 2011; Blundell et al., 2015).

4 Variational Continual Learning in Deep Generative Models

Deep generative models (DGMs) have garnered much recent attention. By passing a simple noise variable (e.g. Gaussian noise) through a deep neural network, these models have been shown to be able to generate realistic images, sounds and videos sequences (Chung et al., 2015; Kingma et al., 2016; Vondrick et al., 2016). Standard approaches for learning DGMs have focused on the batch learning, i.e. the observed instances are assumed to be i.i.d. and are all available at the same time. In this section we extend the VCL framework to encompass variational auto-encoders (VAEs) (Kingma and Welling, 2014; Rezende et al., 2014), a form of DGMs. The approach could be extended to generative adversarial networks (GAN) (Goodfellow et al., 2014b) for which continual learning is an open problem, but see Seff et al. (2017) for an initial attempt.

Consider a model $p(\mathbf{x}|\mathbf{z}, \boldsymbol{\theta})p(\mathbf{z})$, for observed data $\mathbf{x}$ and latent variables $\mathbf{z}$. The prior over latent variables $p(\mathbf{z})$ is typically Gaussian, and the distributional parameters of $p(\mathbf{x}|\mathbf{z}, \boldsymbol{\theta})$ are defined by a deep neural network. For example, if Bernoulli likelihood is used, then $p(\mathbf{x}|\mathbf{z}, \boldsymbol{\theta}) = \text{Bern}(\boldsymbol{f}_{\boldsymbol{\theta}}(\mathbf{z}))$, where $\boldsymbol{f}_{\boldsymbol{\theta}}$ denotes the deep neural network transform and $\boldsymbol{\theta}$ collects all the weight matrices and bias vectors. In the batch setting, given a dataset $\mathcal{D} = \{\mathbf{x}_n\}_{n=1}^N$, the standard VAE approach learns the parameters $\boldsymbol{\theta}$ by approximate maximum likelihood estimation (MLE). This proceeds by maximizing the variational lower bound with respect to $\boldsymbol{\theta}$ and $\boldsymbol{\phi}$:

$$\mathcal{L}_{\text{VAE}}(\boldsymbol{\theta}, \boldsymbol{\phi}) = \sum_{n=1}^{N} \mathbb{E}_{q_{\boldsymbol{\phi}}(\mathbf{z}|\mathbf{x}_n)}\left[\log \frac{p(\mathbf{x}_n|\mathbf{z}, \boldsymbol{\theta})p(\mathbf{z})}{q_{\boldsymbol{\phi}}(\mathbf{z}|\mathbf{x}_n)}\right], \tag{5}$$

where $\boldsymbol{\phi}$ denotes the variational parameters for the "encoder" or the approximate posterior of $\boldsymbol{z}$ given an observation $\boldsymbol{x}_n$.

The approximate MLE approach is unsuitable for the continual learning setting as it does not return parameter uncertainty estimates that are critical for weighting the information learned from old data. So, instead the VCL approach will approximate the full posterior distribution over parameters, $q_t(\boldsymbol{\theta}) \approx p(\boldsymbol{\theta}|\mathcal{D}_{1:t})$, after observing the t-th dataset. Specifically, the approximate posterior q_t is obtained by maximizing the *full* variational lower bound with respect to q_t and $\boldsymbol{\phi}$:

$$\mathcal{L}^t_{\text{VCL}}(q_t(\boldsymbol{\theta}), \boldsymbol{\phi}) = \mathbb{E}_{q_t(\boldsymbol{\theta})} \left\{ \sum_{n=1}^{N_t} \mathbb{E}_{q_{\boldsymbol{\phi}}(\mathbf{z}|\mathbf{x}_t^{(n)})} \left[\log \frac{p(\mathbf{x}_t^{(n)}|\mathbf{z}, \boldsymbol{\theta}) p(\mathbf{z})}{q_{\boldsymbol{\phi}}(\mathbf{z}|\mathbf{x}_t^{(n)})} \right] \right\} - \text{KL}(q_t(\boldsymbol{\theta})||q_{t-1}(\boldsymbol{\theta})), \tag{6}$$

where the encoder network $q_{\boldsymbol{\phi}}(\boldsymbol{z}|\boldsymbol{x}_t^{(n)})$ is parameterized by $\boldsymbol{\phi}$ which is task-specific. It is likely to be beneficial to share (parts of) these encoder networks, but this is not investigated in this paper.

As was the case for multi-head discriminative models, we can split the generative model into shared and task-specific parts. There are two options: (i) the generative models share across tasks the network that generates observations $\mathbf{x}$ from the intermediate-level representations $\mathbf{h}$, but have their own "head network" for generating $\mathbf{h}$ from the latent variables $\mathbf{z}$ (see fig. 1(b)), and (ii) the other way around. In the latter architecture, if the task-specific lower-level network is reasonably deep, the information of the current task can be encoded efficiently in this part of the network, thus effectively ignoring the shared high-level network. Due to this reason, we focus on the former architecture in the experiments where the network is forced to share information between tasks.

5 Related Work

Continual Learning for Deep Discriminative Models: Many neural network continual learning approaches employ regularized maximum likelihood estimation, optimizing objectives of the form:

$$\mathcal{L}^t(\boldsymbol{\theta}) = \textstyle\sum_{n=1}^{N_t} \log p(y_t^{(n)}|\boldsymbol{\theta}, \mathbf{x}_t^{(n)}) - \frac{1}{2}\lambda_t(\boldsymbol{\theta} - \boldsymbol{\theta}_{t-1})^{\text{T}}\Sigma_{t-1}^{-1}(\boldsymbol{\theta} - \boldsymbol{\theta}_{t-1}).$$

Here the regularization biases the new parameter estimates towards those estimated at the previous step $\boldsymbol{\theta}_{t-1}$. λ_t is a user-selected hyper-parameter that controls the overall contribution from previous data and Σ_{t-1} is a matrix (normally diagonal in form) that encodes the relative strength of the regularization on each element of $\boldsymbol{\theta}$. We now discuss specific instances of this scheme:

- **Maximum-likelihood estimation and MAP estimation**: maximum likelihood estimation is recovered when there is no regularization ($\lambda_t = 0$). More generally, the regularization term can be interpreted as a Gaussian prior, $q(\boldsymbol{\theta}|\mathcal{D}_{1:t-1}) = \mathcal{N}(\boldsymbol{\theta}; \boldsymbol{\theta}_{t-1}, \Sigma_{t-1}/\lambda_t)$. The optimization returns the *maximum a posteriori* estimate of the parameters, but this does not directly provide a Σ_t for the next stage. A simple fix is to set $\Sigma_t = \text{I}$ and use cross-validation to find λ_t, but this approximation is often coarse and leads to catastrophic forgetting (Goodfellow et al., 2014a; Kirkpatrick et al., 2017).

- **Laplace Propagation** (Smola et al., 2004): applying Laplace approximation at each step leads to a recursion for Σ_t^{-1}, which is initialized using the covariance of the Gaussian prior,

  $$\Sigma_t^{-1} = \Phi_t + \Sigma_{t-1}^{-1} \text{ where } \Phi_t = -\nabla\nabla_{\boldsymbol{\theta}} \textstyle\sum_{n=1}^{N_t} \log p(y_t^{(n)}|\boldsymbol{\theta}, \mathbf{x}_t^{(n)})\Big|_{\boldsymbol{\theta}=\boldsymbol{\theta}_t} \text{ and } \lambda_t = 1.$$

  To avoid computing the full Hessian of the likelihood, diagonal-Laplace propagation retains only the diagonal terms of Σ_t^{-1}.

- **Elastic Weight Consolidation (EWC)** (Kirkpatrick et al., 2017) builds on diagonal-Laplace propagation by approximating the average Hessian of the likelihoods using well-known identities for the Fisher information:

  $$\Phi_t \approx \text{diag}\left(\textstyle\sum_{n=1}^{N_t} \left(\nabla_{\boldsymbol{\theta}} \log p(y_t^{(n)}|\boldsymbol{\theta}, \mathbf{x}_t^{(n)}) \right)^2 \Big|_{\boldsymbol{\theta}=\boldsymbol{\theta}_t} \right).$$

  EWC also modifies the Laplace regularization, $\frac{1}{2}(\boldsymbol{\theta} - \boldsymbol{\theta}_{t-1})^\intercal(\Sigma_0 + \sum_{t'=1}^{t-1}\Phi_{t'})(\boldsymbol{\theta} - \boldsymbol{\theta}_{t-1})$, introducing hyper-parameters, removing the prior and regularizing to intermediate parameter estimators, rather than just that derived from the last task, $\frac{1}{2}\sum_{t'=1}^{t-1}\lambda_{t'}(\boldsymbol{\theta} - \boldsymbol{\theta}_{t'-1})^\intercal\Phi_{t'}(\boldsymbol{\theta} - \boldsymbol{\theta}_{t'-1})$. This final change is likely to be unnecessary and deleterious in some cases (Huszar, 2017).

- **Synaptic Intelligence (SI)** (Zenke et al., 2017): SI computes Σ_t^{-1} using a measure of the importance of each parameter to each task. Practically, this is achieved by comparing the changing rate of the gradients of the objective and the changing rate of the parameters.

VCL differs from the above methods in several ways. First, unlike MAP, EWC and SI approaches above, it does not have free parameters that need to be tuned on a validation set. This can be especially awkward in the online setting. Second, although the KL regularization penalizes the mean of the approximate posterior through a quadratic cost, a full distribution is retained and needs to be averaged over at training time and at test time. Third, and more generally, VI is generally thought to return better uncertainty estimates than approaches like Laplace method and MAP estimation, and we have argued this is critical for continual learning.

There is a long history of research on approximate Bayesian approaches to training neural networks, including extended Kalman filtering (Singhal and Wu, 1989), Laplace approximation (MacKay, 1992), variational inference (Hinton and Van Camp, 1993; Barber and Bishop, 1998; Graves, 2011; Blundell et al., 2015; Gal and Ghahramani, 2016), sequential Monte Carlo (de Freitas et al., 2000), EP (Hernández-Lobato and Adams, 2015), and approximate Power EP (Hernández-Lobato et al., 2016). These approaches have been focused on batch learning, but the framework described in section 2 also enables them to be applied to continual learning. On the other hand, the online variational inference has been previously explored (Ghahramani and Attias, 2000; Broderick et al., 2013; Bui et al., 2017), but not for neural networks or in the context of complex tasks.

Continual Learning for Deep Generative Models: A naïve continual learning approach for deep generative models would directly apply the VAE algorithm to the new dataset $\mathcal{D}_t$ with the model parameters initialized at the previous parameter values $\boldsymbol{\theta}_{t-1}$. Our experiments show that this approach leads to catastrophic forgetting, in the sense that the generator can only generate instances that are similar to the data points from the most recently observed dataset.

Alternatively, EWC regularization can be added to the VAE objective:

$$\mathcal{L}^t_{\text{EWC}}(\boldsymbol{\theta}, \boldsymbol{\phi}) = \sum_{n=1}^{N_t} \mathbb{E}_{q_{\boldsymbol{\phi}}(\mathbf{z}|\mathbf{x}_t^{(n)})} \left[\log \frac{p(\mathbf{x}_t^{(n)}|\mathbf{z}, \boldsymbol{\theta}) p(\mathbf{z})}{q_{\boldsymbol{\phi}}(\mathbf{z}|\mathbf{x}_t^{(n)})} \right] - \frac{1}{2} \sum_{t'=1}^{t-1} \lambda_{t'} (\boldsymbol{\theta} - \boldsymbol{\theta}_{t'-1})^\intercal \Phi_{t'} (\boldsymbol{\theta} - \boldsymbol{\theta}_{t'-1}).$$

However computing Φ_t requires the gradient $\nabla_{\boldsymbol{\theta}} \log p(\mathbf{x}|\boldsymbol{\theta})$ which is intractable. Instead, we can approximate the marginal likelihood by the variational lower bound, i.e.

$$\Phi_t = \text{diag}\Big(\sum_{n=1}^{N_t} \Big(\nabla_{\boldsymbol{\theta}} \mathbb{E}_{q_{\boldsymbol{\phi}}(\mathbf{z}|\mathbf{x}_t^{(n)})} \big[\log \frac{p(\mathbf{x}_t^{(n)}|\mathbf{z}, \boldsymbol{\theta}) p(\mathbf{z})}{q_{\boldsymbol{\phi}}(\mathbf{z}|\mathbf{x}_t^{(n)})} \big] \Big)^2 \Big|_{\boldsymbol{\theta}=\boldsymbol{\theta}_t} \Big).$$

An importance sampling estimate could also be used using Burda et al. (2016). In our experiments with DGMs, this version of EWC is used as a baseline to compare with VCL.

6 Experiments

6.1 Experiments with Deep Discriminative Models

We consider two continual learning experiments for deep discriminative models: the permuted MNIST experiment and the split MNIST experiment. More details of the experiment settings and an additional experiment are available in the appendix.

Permuted MNIST: This is a popular continual learning benchmark (Goodfellow et al., 2014a; Kirkpatrick et al., 2017; Zenke et al., 2017). The dataset received at each time step $\mathcal{D}_t$ consists of labeled MNIST images whose pixels have undergone a fixed random permutation. We compare VCL to EWC and SI. For all algorithms, we use fully connected single-head networks with two hidden layers, where each layer contains 100 hidden units with ReLU activations. We evaluate three versions of VCL: VCL with no coreset, VCL with a random coreset, and VCL with a coreset selected by the K-center method. For the coresets, we select 200 data points from each task.

Figure 2 compares the average test set accuracy on all observed tasks. From this figure, VCL outperforms the EWC and SI by large margins, even though they benefited from an extensive hyper-parameter search for λ. After 10 tasks, VCL achieves 90% average accuracy, while EWC and SI only achieve 84% and 86% respectively. The results also show that using the coresets alone is not useful for this task, but combining them with VCL leads to a modest improvement over VCL: both random coresets and K-center coresets achieve 93% accuracy.

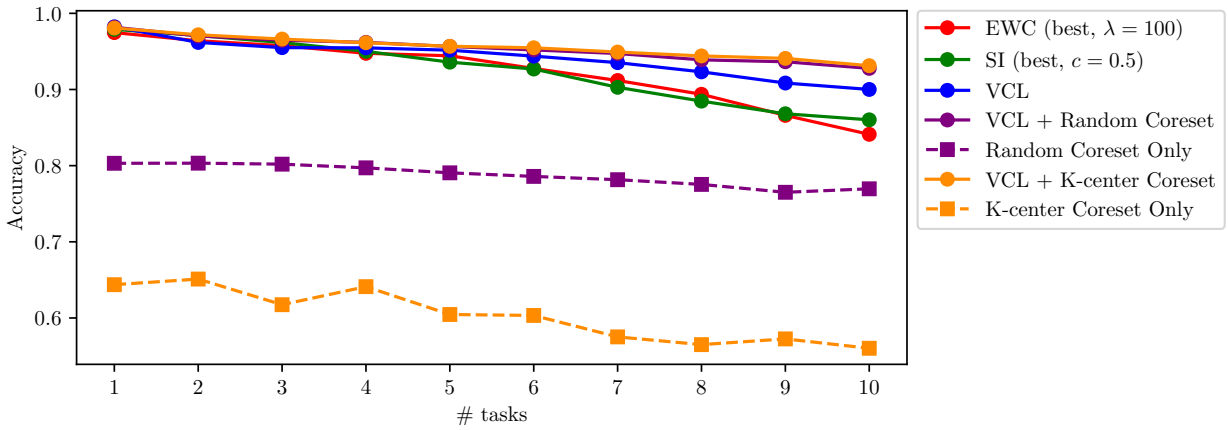

Figure 2: Average test set accuracy on all observed tasks for the Permuted MNIST experiment.

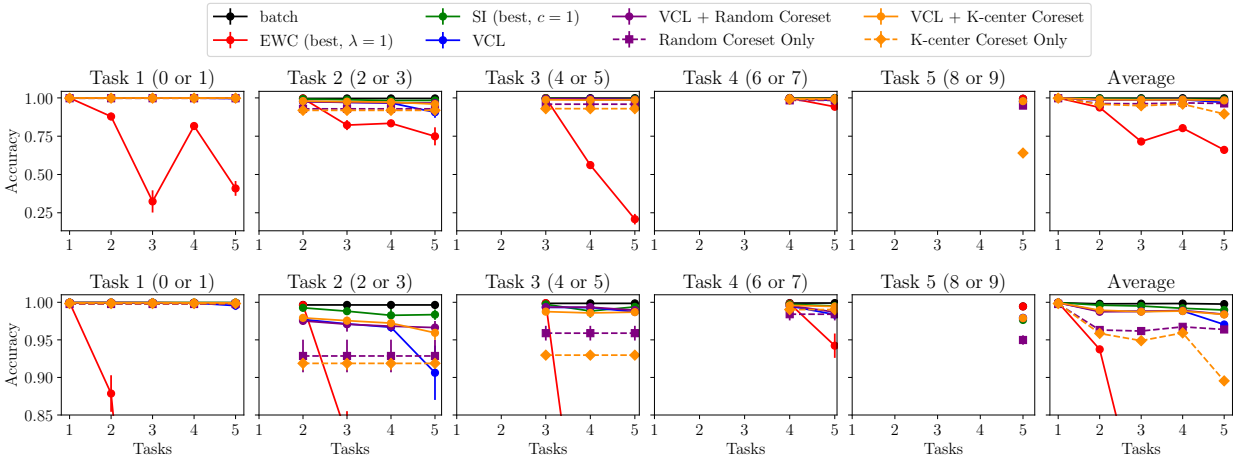

Figure 3: Test set accuracy on all tasks for the Split MNIST experiment. The last column shows the average accuracy over all tasks. The bottom row is a zoomed version of the top row.

Split MNIST: This experiment was used by Zenke et al. (2017) to assess the SI method. Five binary classification tasks from the MNIST dataset arrive in sequence: 0/1, 2/3, 4/5, 6/7, and 8/9. We use fully connected multi-head networks with two hidden layers comprising 256 hidden units with ReLU activations. We compare VCL (with and without coresets) to EWC and SI. For the coresets, 40 data points from each task are selected through random sampling or the K-center method.

Figure 3 compares the test set accuracy on individual tasks (averaged over 10 runs) as well as the accumulated accuracy averaged over tasks (right most column). As an upper bound on the algorithms' performance, we compare to batch VI trained on the full dataset. From this figure, VCL significantly outperforms EWC although it is slightly worse than SI. Again, EWC and SI benefited from a hyper-parameter search for λ, but a value close to 1 performs well in both cases. After 5 tasks, VCL achieves 97.0% average accuracy on all tasks, while EWC and SI attain 63.1% and 98.9% respectively. Adding the coreset improves the performance of VCL to around 98.4% accuracy.

6.2 Experiments with Deep Generative Models

We consider two continual learning experiments for deep generative models: MNIST digit generation and notMNIST (small) character generation. In both cases, ten datasets are received in sequence. For MNIST, the first dataset comprises exclusively of images of the digit zero, the second dataset ones and so on. For

notMNIST (small), the datasets contain the characters A to J in sequence. The generative model consists of shared and task-specific components, each represented by a one hidden layer neural network with 500 hidden units (see fig. 1(b)). The dimensionality of the latent variable $\mathbf{z}$ and the intermediate representation $\mathbf{h}$ are 50 and 500, respectively. We use task-specific encoders that are neural networks with symmetric architectures to the generator.

We compare VCL to naïve online learning using the standard VAE objective and EWC (with hyper-parameters $\lambda = 1, 10, 100$). For full details of the experimental settings, see appendix D. Samples from the generative models attained at different time steps are shown in fig. 4. The naïve online learning method fails catastrophically and so we have not included numerical results in the main text. EWC and VCL manage to remember the previous tasks.

EWC and VCL are quantitatively evaluated using two metrics in fig. 5: an importance sampling estimate of the test log-likelihood (test-LL) using $5,000$ samples and a measure of quality we term "classifier uncertainty". For the latter, we train a discriminative classifier for the digits/alphabets. The quality of generated samples can then be assessed by computing the entropy of the output classification probability vector. A well-trained generator will produce images that are confidently classified resulting in zero entropy. Initially, VCL performs slightly worse in terms of test-LL on the most recent task when compared to EWC. This is likely due to the fact that VCL optimizes a distribution over random weights $\boldsymbol{\theta}$ while EWC computes point estimates, and the latter strategy often produces higher test-LL. However, importantly VCL has a superior long-term memory of previous tasks which leads to better overall performance on both metrics. Again, we note that EWC benefited here from carefully tuning the hyper-parameter. This again reveals a key advantage of the VCL approach: its objective function is hyper-parameter free. Very interestingly, all EWC methods suffer from performance deteriorations when moving from task "digit 0" to "digit 1", probably because these two digits are very different. Future work will investigate continual learning on a sequence of tasks that follows "adversarial ordering", i.e. the ordering that makes the next task maximally different from the current task.

7 Conclusion

Approximate Bayesian inference provides a natural framework for continual learning. VCL, developed in this paper, is an approach in this vein that extends online variational inference to handle more general continual learning tasks and complex neural network models. VCL can be enhanced by including a small episodic memory that leverages coreset algorithms from statistics. We demonstrated how the VCL framework can be applied to both discriminative and generative models. Experimental results showed state-of-the-art performance when compared to previous continual learning approaches, even though VCL has no free parameters in its objective function. Future work should explore alternative approximate inference methods using the same framework and also develop more sophisticated episodic memories. Finally, we note that VCL is ideally suited for efficient model refinement in sequential decision making problems, such as RL and active learning.

Acknowledgments

The authors would like to thank Brian Trippe, Siddharth Swaroop, and Matej Balog for insightful comments and discussion. Cuong V. Nguyen is supported by EPSRC grant EP/M0269571. Yingzhen Li is supported by the Schlumberger FFTF Fellowship. Thang D. Bui is supported by the Google European Doctoral Fellowship. Richard E. Turner is supported by Google as well as EPSRC grants EP/M0269571 and EP/L000776/1.

References

Olivier Bachem, Mario Lucic, and Andreas Krause. Coresets for nonparametric estimation – the case of DP-means. In *International Conference on Machine Learning*, 2015.

Bart Bakker and Tom Heskes. Task clustering and gating for Bayesian multitask learning. *Journal of Machine Learning Research*, 2003.

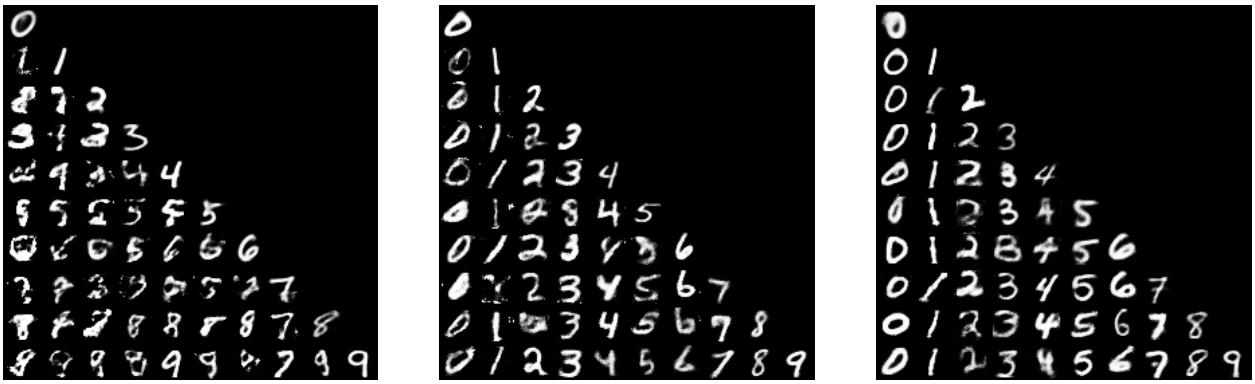

(a) MNIST, naive. (b) MNIST, EWC, $\lambda = 10$. (c) MNIST, VCL.

(d) notMNIST, naive. (e) notMNIST, EWC, $\lambda = 100$. (f) notMNIST, VCL.

Figure 4: Generated images from each of the generators after training. Each of the columns shows the images generated from a specific task's generator, and each of the lines shows the generations from generators of all trained tasks. Clearly the naive approach suffers from catastrophic forgetting, while EWC and VCL successfully remember previous tasks.

David Barber and Christopher M. Bishop. Ensemble learning in Bayesian neural networks. In *Neural Networks and Machine Learning*, 1998.

Charles Blundell, Julien Cornebise, Koray Kavukcuoglu, and Daan Wierstra. Weight uncertainty in neural network. In *International Conference on Machine Learning*, 2015.

Tamara Broderick, Nicholas Boyd, Andre Wibisono, Ashia C. Wilson, and Michael I. Jordan. Streaming variational Bayes. In *Advances in Neural Information Processing Systems*, 2013.

Thang Bui, Daniel Hernández-Lobato, Jose Hernandez-Lobato, Yingzhen Li, and Richard Turner. Deep Gaussian processes for regression using approximate expectation propagation. In *International Conference on Machine Learning*, 2016.

Thang D. Bui, Cuong V. Nguyen, and Richard E. Turner. Streaming sparse Gaussian process approximations. In *Advances in Neural Information Processing Systems*, 2017.

Yuri Burda, Roger Grosse, and Ruslan Salakhutdinov. Importance weighted autoencoders. In *International Conference on Learning Representations*, 2016.

Junyoung Chung, Kyle Kastner, Laurent Dinh, Kratarth Goel, Aaron C. Courville, and Yoshua Bengio. A recurrent latent variable model for sequential data. In *Advances in Neural Information Processing Systems*, 2015.

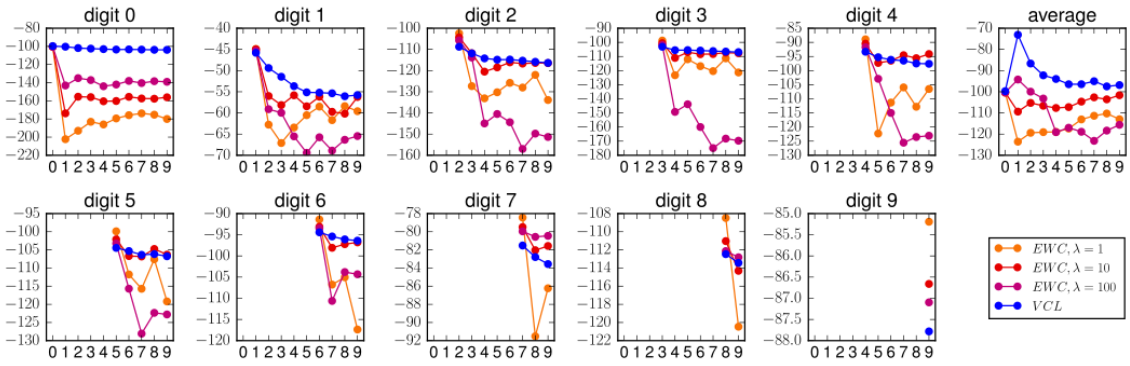

(a) Test-LL results on MNIST. The higher the better.

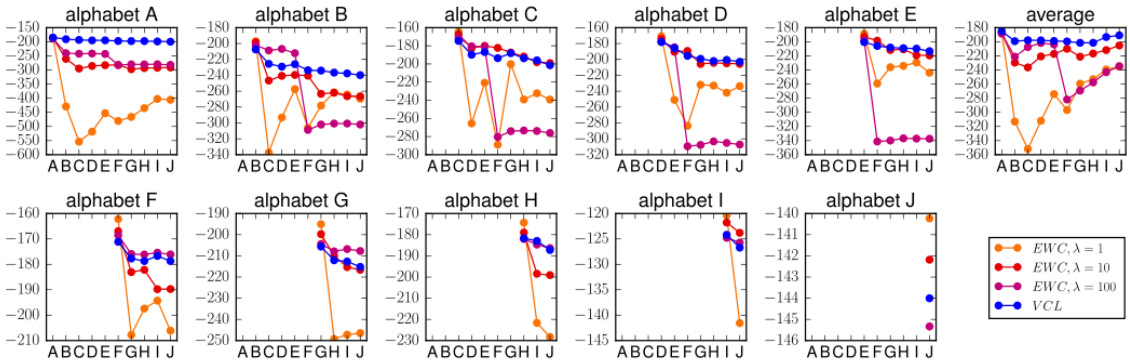

(b) Test-LL results on notMNIST. The higher the better.

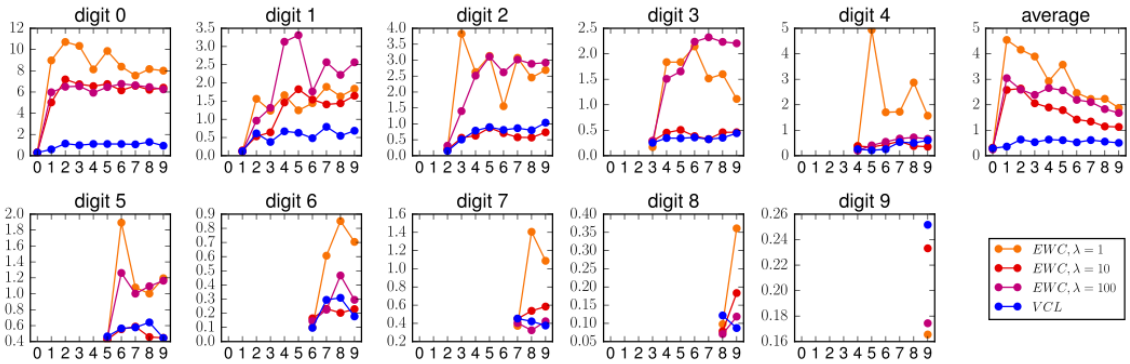

(c) Classifier uncertainty on MNIST. The lower the better.

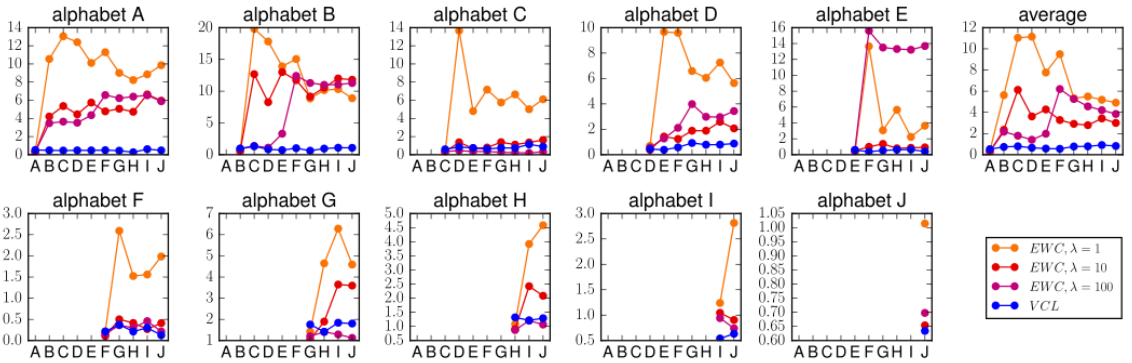

(d) Classifier uncertainty on notMNIST. The lower the better.

Figure 5: Quantitative results for continual learning for DGMs. See main text for a discussion.

Nando de Freitas, Mahesan Niranjan, Andrew H. Gee, and Arnaud Doucet. Sequential Monte Carlo methods to train neural network models. *Neural Computation*, 2000.

Yarin Gal and Zoubin Ghahramani. Dropout as a Bayesian approximation: Representing model uncertainty in deep learning. In *International Conference on Machine Learning*, 2016.

Zoubin Ghahramani and H. Attias. Online variational Bayesian learning. In *NIPS Workshop on Online Learning*, 2000.

Teofilo F. Gonzalez. Clustering to minimize the maximum intercluster distance. *Theoretical Computer Science*, 1985.

Ian J. Goodfellow, Mehdi Mirza, Da Xiao, Aaron Courville, and Yoshua Bengio. An empirical investigation of catastrophic forgetting in gradient-based neural networks. In *International Conference on Learning Representations*, 2014a.

Ian J. Goodfellow, Jean Pouget-Abadie, Mehdi Mirza, Bing Xu, David Warde-Farley, Sherjil Ozair, Aaron Courville, and Yoshua Bengio. Generative adversarial nets. In *Advances in Neural Information Processing Systems*, 2014b.

Alex Graves. Practical variational inference for neural networks. In *Advances in Neural Information Processing Systems*, 2011.

José Miguel Hernández-Lobato and Ryan P. Adams. Probabilistic backpropagation for scalable learning of Bayesian neural networks. In *International Conference on Machine Learning*, 2015.

José Miguel Hernández-Lobato, Yingzhen Li, Mark Rowland, Daniel Hernández-Lobato, Thang D. Bui, and Richard E. Turner. Black-box α-divergence minimization. In *International Conference on Machine Learning*, 2016.

Geoffrey E. Hinton and Drew Van Camp. Keeping the neural networks simple by minimizing the description length of the weights. In *Conference on Computational Learning Theory*, 1993.

Jonathan Huggins, Trevor Campbell, and Tamara Broderick. Coresets for scalable Bayesian logistic regression. In *Advances in Neural Information Processing Systems*, 2016.

Ferenc Huszar. Comment on "Overcoming catastrophic forgetting in NNs": Are multiple penalties needed?, 2017. URL goo.gl/AgdRTN.

Diederik Kingma and Jimmy Ba. Adam: A method for stochastic optimization. In *International Conference on Learning Representations*, 2015.

Diederik P. Kingma and Max Welling. Stochastic gradient VB and the variational auto-encoder. In *International Conference on Learning Representations*, 2014.

Diederik P. Kingma, Tim Salimans, Rafal Jozefowicz, Xi Chen, Ilya Sutskever, and Max Welling. Improved variational inference with inverse autoregressive flow. In *Advances in Neural Information Processing Systems*, 2016.

James Kirkpatrick, Razvan Pascanu, Neil Rabinowitz, Joel Veness, Guillaume Desjardins, Andrei A. Rusu, Kieran Milan, John Quan, Tiago Ramalho, Agnieszka Grabska-Barwinska, Demis Hassabis, Claudia Clopath, Dharshan Kumaran, and Raia Hadsell. Overcoming catastrophic forgetting in neural networks. *Proceedings of the National Academy of Sciences*, 2017.

Sang-Woo Lee, Jin-Hwa Kim, Jung-Woo Ha, and Byoung-Tak Zhang. Overcoming catastrophic forgetting by incremental moment matching. In *Advances in Neural Information Processing Systems*, 2017.

Zhizhong Li and Derek Hoiem. Learning without forgetting. In *European Conference on Computer Vision*, 2016.

Jun S. Liu and Rong Chen. Sequential Monte Carlo methods for dynamic systems. *Journal of the American Statistical Association*, 1998.

David Lopez-Paz and Marc'Aurelio Ranzato. Gradient episodic memory for continual learning. In *Advances in Neural Information Processing Systems*, 2017.

David J.C. MacKay. A practical Bayesian framework for backpropagation networks. *Neural Computation*, 1992.

Peter S. Maybeck. *Stochastic models, estimation, and control*. Academic Press, 1982.

Michael McCloskey and Neal J. Cohen. Catastrophic interference in connectionist networks: The sequential learning problem. *Psychology of Learning and Motivation*, 1989.

Manfred Opper and Cédric Archambeau. The variational Gaussian approximation revisited. *Neural Computation*, 2009.

Roger Ratcliff. Connectionist models of recognition memory: Constraints imposed by learning and forgetting functions. *Psychological Review*, 1990.

Danilo J. Rezende, Shakir Mohamed, and Daan Wierstra. Stochastic backpropagation and approximate inference in deep generative models. In *International Conference on Machine Learning*, 2014.

Mark B. Ring. CHILD: A first step towards continual learning. *Machine Learning*, 1997.

Andrei A. Rusu, Neil C. Rabinowitz, Guillaume Desjardins, Hubert Soyer, James Kirkpatrick, Koray Kavukcuoglu, Razvan Pascanu, and Raia Hadsell. Progressive neural networks. *arXiv:1606.04671*, 2016.

Tim Salimans and David A. Knowles. Fixed-form variational posterior approximation through stochastic linear regression. *Bayesian Analysis*, 2013.

Masa-Aki Sato. Online model selection based on the variational Bayes. *Neural Computation*, 2001.

Jeffrey C. Schlimmer and Douglas Fisher. A case study of incremental concept induction. In *The National Conference on Artificial Intelligence*, 1986.

Ari Seff, Alex Beatson, Daniel Suo, and Han Liu. Continual learning in generative adversarial nets. *arXiv:1705.08395*, 2017.

Sharad Singhal and Lance Wu. Training multilayer perceptrons with the extended Kalman algorithm. In *Advances in Neural Information Processing Systems*, 1989.

Alex J. Smola, S.V.N. Vishwanathan, and Eleazar Eskin. Laplace propagation. In *Advances in Neural Information Processing Systems*, 2004.

Richard S. Sutton and Steven D. Whitehead. Online learning with random representations. In *International Conference on Machine Learning*, 1993.

Carl Vondrick, Hamed Pirsiavash, and Antonio Torralba. Generating videos with scene dynamics. In *Advances In Neural Information Processing Systems*, 2016.

Friedemann Zenke, Ben Poole, and Surya Ganguli. Continual learning through synaptic intelligence. In *International Conference on Machine Learning*, 2017.

Appendix

A Experiment Settings for the Permuted MNIST Experiment

In this experiment, we use fully connected single-head networks with two hidden layers, where each layer contains 100 hidden units with ReLU activations. The metric used for comparison is the test set accuracy on all observed tasks. We train all the models using the Adam optimizer (Kingma and Ba, 2015) with learning rate 10^{-3} since we found that it works best for all models. All the VCL algorithms are trained with batch size 256 and 100 epochs. For all the algorithms with coresets, we choose 200 examples from each task to include into the coresets. The algorithms that use only the coresets are trained using the VFE method with batch size equal to the coreset size and 100 epochs.

We compare the performance of the SI method that uses $c = 0.01, 0.1, 0.5, 1, 2$, where c is the regularization strength hyper-parameter (see fig. 6). Following the settings in (Zenke et al., 2017), we train these models with batch size 256 and 20 epochs. The best value of c for this method is 0.5, so we use this value as the baseline for our experiment.

We also compare the performance of the EWC method that uses $\lambda = 1, 10, 10^2, 10^3, 10^4$, where λ is the regularization strength hyper-parameter (see fig. 7). The models are trained without drop-out and with batch size 200 and 20 epochs. We approximate the Fisher information matrix using 600 random samples drawn from the current dataset. The best value of λ for this method is 10^2, thus we use this value as the baseline for our experiment.

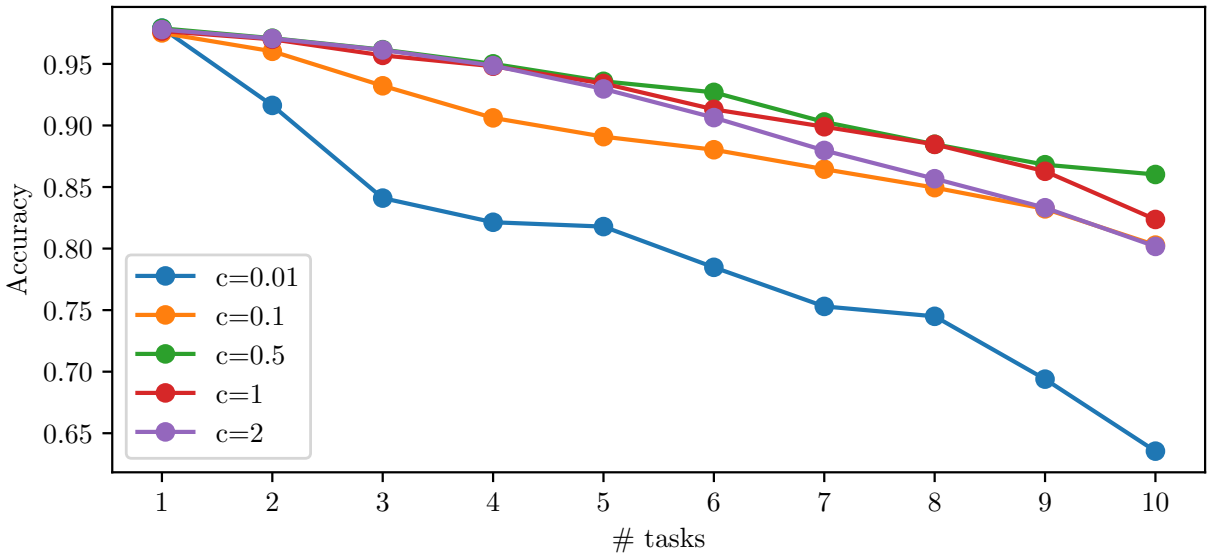

Figure 6: Comparison of the SI method (Zenke et al., 2017) with different regularization strength hyper-parameter (c) values in the Permuted MNIST experiment.

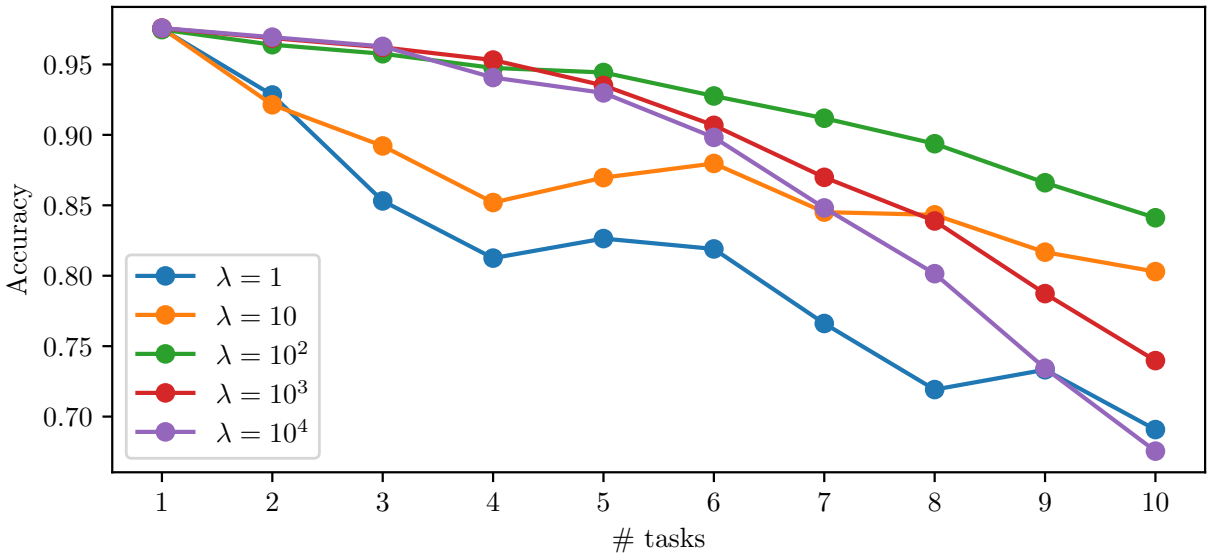

Figure 7: Comparison of the EWC method (Kirkpatrick et al., 2017) with different regularization strength hyper-parameter (λ) values in the Permuted MNIST experiment.

B Experiment Settings for the Split MNIST Experiment

In this experiment, we use fully connected multi-head networks with two hidden layers, each of which contains 256 hidden units with ReLU activations. At each time step, we compare the test set accuracy of the current model on all observed tasks separately. We also plot the average accuracy over all tasks in the last column of fig. 3. All the results for this experiment are the averages over 10 runs of the algorithms with different random seeds.

We also use the Adam optimizer with learning rate 10^{-3} for all models in this experiment. All the VCL algorithms are trained with batch size equal to the size of the training set and 120 epochs. For the coresets, we choose 40 examples from each task to include into the coresets. In this experiment, the final approximate posterior used for prediction in eq. (3) is computed for each task separately using the coreset points corresponding to the task. The algorithms that use only the coresets are trained using the VFE method with batch size equal to the coreset size and 120 epochs.

We compare the performance of the SI method with $c = 0.01, 0.1, 1, 2, 3$ and use the best value $c = 1$ as the baseline for our experiment (see fig. 8). We also compare the EWC method with both single-head and multi-head models and $\lambda = 1, 10, 10^2, 10^3, 10^4$ (see fig. 9). The figure shows that the multi-head models work better than the single-head models for EWC, and the performance is insensitive to the choice of λ. Thus, we use the multi-head model with $\lambda = 1$ as the EWC baseline for our experiment.

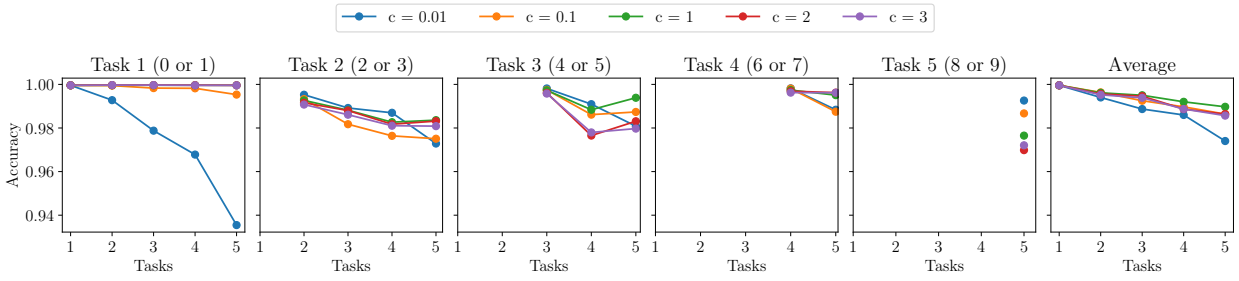

Figure 8: Comparison of the SI method (Zenke et al., 2017) with different regularization strength hyper-parameter (c) values in the Split MNIST experiment.

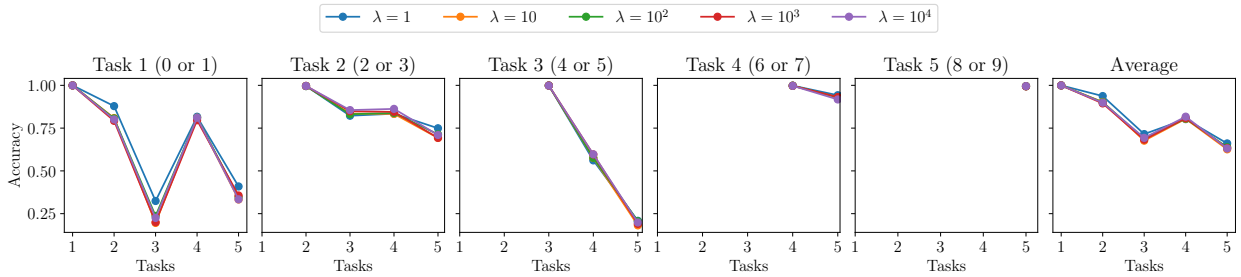

(a) Multi-head model.

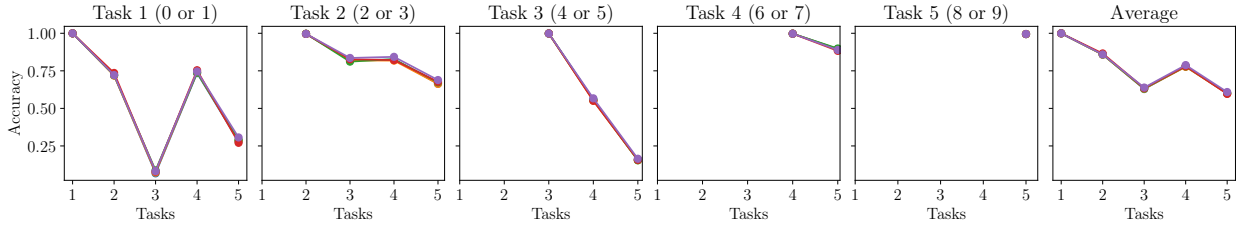

(b) Single-head model.

Figure 9: Comparison of the EWC method (Kirkpatrick et al., 2017) with different regularization strength hyper-parameter (λ) values in the Split MNIST experiment.

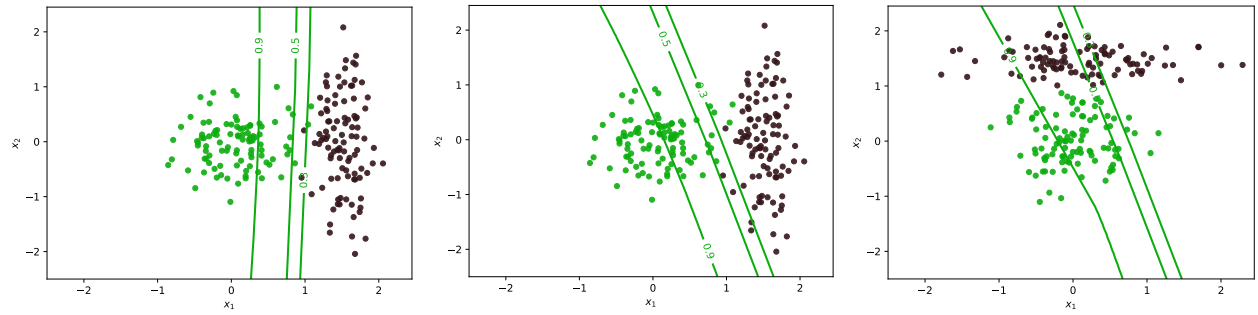

(a) Multi-head EWC model.

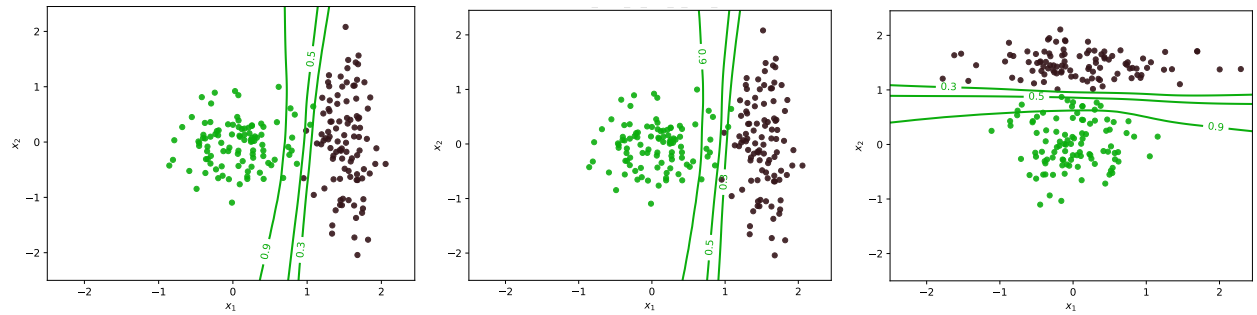

(b) Multi-head VCL model.

Figure 10: Comparison of VCL and EWC on a toy 2D dataset. The first column shows the contours of the prediction probabilities after observing the first task. The second and third columns show the contours for the first and the second tasks respectively after observing the second task.

(a) MNIST, naive. (b) MNIST, EWC, $\lambda = 10$. (c) MNIST, VCL.

(d) notMNIST, naive. (e) notMNIST, EWC, $\lambda = 100$. (f) notMNIST, VCL.

Figure 11: Generated images from each of the generators after last task training. Each rows show the samples from the corresponding task-specific generator.

C Additional Experiment on a Toy 2D Dataset

In this small experiment, we compare VCL and EWC on a toy 2D dataset. The experiment has two sequential binary classification tasks. The first task contains two classes generated from two Gaussian distributions. The data points (with green and black classes) for this tasks are shown in the first column of fig. 10. The second task contains two classes also generated from two Gaussian distributions. The green class for this task has the same input distribution as the first task, while the input distribution for the black class is different. The data points for this task are shown in the second and third columns of fig. 10. Each task contains 200 data points with 100 data points in each class.

We compare the multi-head models trained by VCL and EWC on these two tasks. In this experiment, we use fully connected networks with one hidden layers containing 20 hidden units with ReLU activations. The first column of fig. 10 shows the contours of the prediction probabilities after observing the first task, and both methods perform reasonably well for this task. However, after observing the second task, the EWC method fails to learn the classifiers for both tasks, while the VCL method are still able to learn good classifiers for them.

D Experiment Settings and More Samples from the DGMs

Figure 11 shows additional images generated from the generators described in the main text. In this experiment, the learning rates and numbers of optimization epochs are tuned on separate training of each tasks. This gives a learning rate of 10^{-4} and the number of epochs 200 for MNIST and 400 for notMNIST. For the VCL approach, the parameters of $q_t(\boldsymbol{\theta})$ are initialized to have the same mean as $q_{t-1}(\boldsymbol{\theta})$ and the log

standard deviation to 10^{-6}.

The generative model consists of shared and task-specific components, each represented by a one hidden layer neural network with 500 hidden units (see fig. 1(b)). The dimensionality of the latent variable $\mathbf{z}$ and the intermediate representation $\mathbf{h}$ are 50 and 500, respectively. We use task-specific encoders that are neural networks with symmetric architectures to the generator.

E Memory of a Linear Regression Model Trained with VCL on Random Patterns

In many probabilistic models with conjugate priors, the exact posterior of the parameters/latent variables can be obtained. For example, a Bayesian linear regression model with a Gaussian prior over the parameters and a Gaussian observation model has a Gaussian posterior. If we insist on using a diagonal Gaussian approximation to this posterior and use either the variational free energy method or the Laplace approximation, we will end up at the same solution – a Gaussian distribution with the same mean as that of the exact posterior and the diagonal precisions being the diagonal precisions of the exact posterior. Consequently, the online variational Gaussian approximation will give the same result to that given by the online Laplace approximation. However, when a diagonal Gaussian approximation is used, the batch and sequential solutions are different.

In the following, we will explicitly detail the sequential variational updates for a Bayesian linear regression model to associate *random binary* patterns to *binary* outcomes (Kirkpatrick et al., 2017), and show its relationship to the online Laplace approximation and the EWC approach of Kirkpatrick et al. (2017). The task consists of associating a random D-dimensional binary vectors $\mathbf{x}_t$ to a random binary output y_t by learning a weight vector W. Note that the possible values of the features and outputs are 1 and -1, and not 0 and 1. We also assume that the model sees only one input-output pair, $\{\mathbf{x}_t, y_t\}$ at the t-th time step and the previous approximate posterior $q_{t-1}(W) = \prod_{d=1}^{D} \mathcal{N}(w_d; m_{t-1,d}, v_{t-1,d})$, and that the observation noise variance σ_y^2 is fixed. The variational updates for the mean and precisions are available in closed-form as follows:

$$\mathbf{m}_t = \left[\mathrm{I} + \mathbf{V}_{t-1}\frac{\mathbf{x}_t\mathbf{x}_t^\intercal}{\sigma_y^2}\right]^{-1}\left[\mathbf{V}_{t-1}\frac{\mathbf{x}_t y_t^\intercal}{\sigma_y^2} + \mathbf{m}_{t-1}\right], \tag{7}$$

$$v_{t,d}^{-1} = v_{t-1,d}^{-1} + \frac{x_{t,d}^2}{\sigma_y^2} \quad \text{for} \quad d = 1, 2, \ldots, D. \tag{8}$$

By further assuming that $\sigma_y = 1$ and $\|\mathbf{x}_t\|_2 = 1$, the equations above become:

$$\mathbf{m}_t = \left[\mathrm{I} - \frac{\bar{\mathbf{x}}_t\bar{\mathbf{x}}_t^\intercal}{1 + v_0^{-1} + \frac{t}{D}}\right]\mathbf{m}_{t-1} + \frac{\bar{\mathbf{x}}}{1 + v_0^{-1} + \frac{t}{D}}, \tag{9}$$

$$v_{t,d}^{-1} = v_{0,d}^{-1} + \frac{t}{D} \quad \text{for} \quad d = 1, 2, \ldots, D, \tag{10}$$

where $\bar{\mathbf{x}}_t = y_t\mathbf{x}_t$. When $v_{0,d}^{-1} = 0$, i.e. the prior is ignored, the update for the mean above is exactly equation **S4** in the supplementary material of Kirkpatrick et al. (2017). Therefore, in this case, the memory of the network trained by online variational inference is identical to that of the online Laplace method, provided in (Kirkpatrick et al., 2017). These methods differ, in practice, when the prior is not ignore or when the parameter regularization constraints are accumulated as discussed in the main text. This equivalence also does not hold in the general case, as discussed by Opper and Archambeau (2009) that the Gaussian variational approximation is like an *averaged and smoothed* Laplace approximation.